Journal of
Computational and Theoretical Nanoscience
Vol. 7, 571–576, 2010

Control of Nanoparticle Growth in High Temperature Reactor: Application of Reduced Population Balance Model

Oluranti Sadiku* and Andrei Kolesnikov

Department of Chemical and Metallurgical Engineering, Faculty of Engineering and the Built Environment, Tshwane University of Technology, Pretoria 0001, South Africa

Aerosol processes often are modeled using the population balance equation (PBE). This article presents a study on the simulation of particle size distribution during nanoparticle growth with simultaneous chemical reaction, nucleation, condensation and coagulation. The method used to reduce the population balance model is the method of moments. Under the assumption of lognormal aerosol size distribution, the method of moments was employed to reduce the original model into a set of first-order ODE's (ordinary differential equations) that accurately reproduce important dynamics of aerosol process. The objective of this study is to investigate if we can use the reduced population balance model for the control of nanoparticle size distribution. The numerical result shows there is a dependence of the average particle diameter on the wall temperatures and the model can thus be used as a basis to synthesize a feedback controller where manipulated variable is the wall temperature of the reactor and the control variable the aerosol size distribution at the outlet of the reactor.

Keywords: Population Balance Equation, Method of Moments, Particle Size Distribution and Average Particle Diameter.

1. INTRODUCTION

Physical characterization of aerosol nanoparticles is critical to the advancement of the underlying science and practical development of nanotechnologies. Nanoparticle size must be tightly controlled to take full advantage of quantum size effects in photonic applications, and agglomeration must be prevented. Agglomeration can only be prevented if the number concentrations are tightly controlled, and this requires that the rate of new particle formation be quantitatively determined. The aerosol system is characterized by large number of interacting particles which differ with respect to certain physical and/or chemical properties such as particle size, shape, morphology, porosity and molecular weight, which in turn, determine the physicochemical and mechanical properties of the final product.[2, 3] Aerosol growth occurs in stages, beginning with the gas phase chemical reaction of the reactants to produce monomers or molecules of the condensable species.[1] Modelling particles with specific properties and morphologies requires tools, which are capable of yielding accurate prediction of particle size, composition and shape. To do this, methodologies that are able to capture the hydrothermal and hydrochemical interactions between the fluid and particles fields are needed. The dynamic of nanoparticle growth is captured by the application of population balance equation (PBE) model which is a valuable means for simulating nanoparticle formation processes.

The industrial importance of nanoparticles and the realization that the physiochemical and mechanical properties of materials made with particulate depends heavily on the characteristics of the underlying particle size distribution (PSD) have motivated significant research attention over the years on modeling and prediction of the production of particles.[4] Debra and Sonia[5] described a single moment sectional model to simulate the evolution of an aerosol distribution that contains more than one chemical component. The proposed method is based on dividing the particle domain into X sections with time variant sections boundaries. Ashish and Christofides[6] used the sectional model to divide the continuous particle size distribution (PSD) into a finite number of sections within which the size distribution function is assumed to be constant. Suddah and Mark[7] used the sectional method of moment to approximate the

*Author to whom correspondence should be addressed.

continuous size distribution by a finite number of sections or bins within which one numerically conserved aerosol property is held constant.

An alternative to sectional methods are the more sophisticated finite element methods. In the finite element approach, the solution of the population balance is expanded in series of polynomials. For the coefficients of this expansion, a set of equations has to be solved and this is obtained by inserting the expansion into the population balance equation. Various methods can be derived by different nodes, functions, and time stepping schemes. The mathematical discipline of functional analysis provides the theoretical framework with which errors can be estimated. This is of course a very attractive feature of finite element methods. Baker and Christofides[8] proposed a finite-dimensional approximation and control of nonlinear parabolic partial differential equation (PDE) systems by combining Galerkin's method with the concept of approximate initial manifolds, known as non-linear Galerkin's method. Alexopoulos and Kiparissides[9] used orthogonal collection of finite element methods to solve a continuous form of general population balance equation (PBE).

Another alternative to sectional methods for solving the population balance equation are Monte Carlo (MC) methods. They are easy to implement, can account for fluctuations, and can easily incorporate several internal coordinates. In the case of nanoparticle modelling, the number of particles is so large that the fluctuations in particle numbers can be neglected. The kinetic Monte Carlo (KMC) method is used to estimate and control methodologies for surface properties (e.g., surface roughness). Monte Carlo methods can be easily extended to multiple internal coordinates and for this reason they have been employed to simulate various systems of nanoparticles. Akhtar et al.[10] included two internal coordinates to describe the restructuring of the particles and showed the time evolution of mass fractal dimension.

The least squares method (LSM) is a well-established technique for solving a wide range of mathematical problems .The basic idea in the LSM is to minimize the integral of the square of the residual over the computational domain, in the case when the exact solutions are sufficiently smooth the convergence rate is exponential. Daora and Jakobosen[11] applied the least square method to solve the population balance equation.

The method of moments (MOM) is computationally the most efficient approach to obtain a numerical approximation to the moments of population balance. For this reason, this method is often used when simulating problems where transport of particles in a flow with complex geometry is essential. The dominant dynamic behaviour of many aerosol processes can be accurately captured by a model that describes the evolution of the three leading moments of aerosol size distribution.[12] The aim of this work is to investigate if we can use the reduced population balance model for the control of nanoparticle size distribution. The measurement of particle size distribution is a distinguishing feature in production of nanoparticles because the particle size provides the critical link between the product quality indices and the operating variables.[1] Thus, the ability to effectively control the shape of the PSD is essential for regulating the end product quality of the process. Many applications require a close control of this distributed particle length scale in order to achieve the highest performance.

2. PROCESS DESCRIPTION

The premixed preheated reactants (titanium tetrachloride and oxygen gas) are injected into the reactor where following exothermic reaction takes place. The products of these reactions are titania monomers and chlorine gas.

$$TiCl_4(g) + O_2(g) \rightarrow TiO_2(s) + 2Cl_2(g) \tag{1}$$

The size of a single TiO_2 molecule (monomer) is larger than the thermodynamic critical cluster size. As a result the difference between chemical reaction and nucleation cannot be noticed, thereby implying that the rapid chemical reaction leads to nucleation burst. The coagulation of TiO_2 monomers leads to an increase in the average particle size and a decrease in particle concentration.

2.1. Population Balance Model

The population balance equation consists of the following nonlinear partial integro-differential equation.[3]

$$\begin{aligned}\frac{\partial n}{\partial t} + \frac{\partial(G(v,z,\bar{x})n)}{\partial v} + c_z\frac{\partial n}{\partial z} - I(v^*)\delta(v-v^*) \\ = \frac{1}{2}\int_o^v \beta(\tilde{v}, v-\tilde{v}, \bar{x})n(\tilde{v},z,t)n(v-\tilde{v},z,t)\,d\tilde{v} \\ - n(v,z,t)\int_o^\infty \beta(v,\tilde{v})n(\tilde{v},z,t)\,d\tilde{v}\end{aligned} \tag{2}$$

The first term on the left hand side of Eq. (2) describe the change in the number concentration of particle volume interval v, $v+dv$ and in the spatial interval z. $z+dz$, $n(v,z,t)$ denotes the particle size distribution function, v is particle volume, t is time, $z \in [0, L]$ is the spatial coordinate, L is the length of the process. The second term on the left hand side gives the loss or gain of particles by condensational growth, the third term on the left hand side which is $c_z \partial n/\partial z$ corresponds to the convective transport of aerosol particles at fluid velocity c_z and the fourth term on the left hand side accounts for the formation of new particles of critical volume v^* by nucleation rate I. $I(v^*)\delta(v-v^*)$, also accounts for gain and loss of particles by condensation. $G(v,z,\bar{x})$, $I(v^*)$ and $\beta(\tilde{v}, v-\tilde{v}, \tilde{x})$ are the nonlinear scalar functions and δ is the standard Dirac function. The mass and energy balance model which predicts the spatio-temporal evolution of the concentrations of

species and temperature of the gas phase given by Ashish and Panagiotis[14] has the following form:

$$\frac{d\bar{x}}{dt} = \bar{A}\frac{d\bar{x}}{dz} + \bar{f}(\bar{x}) + \bar{g}(\bar{x})b(z)u(t) + \tilde{A}\int_0^\infty a(\eta, v, x)\,dv \quad (3)$$

where $\bar{x}(z, t)$ is an n-dimensional vector of state variables that depends on space and time, $\bar{A}$, $\tilde{A}$ are constant matrices, $\bar{f}(\bar{x})$, $\bar{g}(\bar{x})$, $a(\eta, v, x)$ are nonlinear vector functions, $u(t)$ is the axially distributed manipulated input (e.g., wall temperatures, Tw_1 and Tw_2) and $b(z)$ is a known function which determines how control action $u(t)$, is distributed in space. The last term on the right hand side of Eq. (3) accounts for mass and heat transfer from the continuous phase to all the particles in population. The gain and loss of particles by Brownian coagulation is described by the first and second term on the right hand side of Eq. (2) respectively.

$$\frac{1}{2}\int_o^v \beta(\tilde{v}, v-\tilde{v}, \bar{x})n(\tilde{v}, z, t)n(v-\tilde{v}, z, t)\,d\tilde{v}$$
$$-\, n(v, z, t)\int_o^\infty \beta(v, \tilde{v})n(\tilde{v}, z, t)\,d\tilde{v} \quad (4)$$

$G(v, z, \bar{x})$ and β are the condensational growth and collision frequency function, respectively for which two different expressions are used for free molecule size and continuum size regimes.[13] The free molecule size regime takes the following form:

$$G_{FM}(\bar{x}, v, z) = B_1 v^{1/3}(S-1), \quad \text{where}$$
$$B_1 = (36\pi)^{1/3} v_1 n_s (k_B T/2\pi m_1)^{1/2}$$
$$\beta_{FM}(\bar{x}, v, z) = B_2\left(\frac{1}{v} + \frac{1}{v}\right)^{1/2}(v^{1/3} + \bar{v}^{1/3})^2$$
$$B_2 = (3/4\pi)^{1/6}(6k_B T v_1/m_1)^{1/2} \quad (5)$$

And the continuum size regime takes the following form:

$$G_C(\bar{x}, v, z) = B_3 v^{1/3}(S-1) \quad \text{where}$$
$$B_3 = (48\pi^2)^{1/3} D v_1 n_s, \quad D = \lambda(8k_B T/\pi m_1)^{1/2}/3$$
$$\beta_C = B_4\left(\frac{C(v)}{v^{1/3}} + \frac{C(\bar{v})}{\bar{v}^{1/3}}\right)(v^{1/3} + \bar{v}^{1/3}), \quad B_4 = \frac{2k_B T}{3\mu} \quad (6)$$

In Eqs. (5) and (6), T is the temperature, S is the saturation ratio, D is the condensable vapour diffusivity, λ is the mean free path of the gas, μ is the fluid viscosity, n_s is the monomer concentration at saturation. ($n_s = P_s/k_B T$, where P_s is the saturation pressure), m_1 is the monomer mass, v_1 is the monomer volume, r is the particle radius, $C(v) = 1 + B_5\lambda/r$ is the Cunningham correction factor and $B_5 = 1.257$. Lastly, the nucleation rate $I(v^*)$ is assumed to follow the classical Becker-Doring theory given by the expression below (Pratisinis).[15]

$$I = n_s^2 s_1 (k_B T/2\pi m_1)^{1/2} S^2 (2/9\pi)^{1/3} \sum^{1/2} \exp(-k^* InS/2) \quad (7)$$

where s_1 is the monomer surface area and k^* is the number of monomer in critical nucleus and is given by:

$$k^* = \frac{\pi}{6}\left(\frac{4\sum}{InS}\right)^3 \quad (8)$$

Where $\sum = \gamma v_1^{2/3}/k_B T$ and is the surface tension.

3. LOGNORMAL AEROSOL SIZE DISTRIBUTION

The population balance model in Eq. (2) is highly complex and does not allow the direct use for numerical computation of the size distribution in real-time. To overcome this problem and to accelerate the computations, method of moments was employed to reduce the population balance model to a set of ODEs for the moments of the size distribution. In order to describe the spatio-temporal evolution of the three leading moments of the volume distribution (which describes the exact evolution of the lognormal aerosol size), a lognormal function was employed in moment model, which was applied to population balance model.

3.1. Moment Model

We assumed that the aerosol size distribution can be adequately represented by lognormal function which is described as:

$$n(v, z, t) = \frac{1}{3v}\frac{1}{\sqrt{2\pi}In\sigma}\exp\left[-\frac{In^2(v/v_g)}{18In^2\sigma}\right] \quad (9)$$

where v_g, is the geometric average particle volume and σ is the standard deviation. The kth moment of the distribution is defined as:

$$M_k(t) = \int_0^\infty v^k n(v, z, t)\,dv \quad (10)$$

According to the properties of a lognormal function, any moment can be written in terms of M_0, v_g, and σ as follows:

$$M_k = M_0 v_g^k \exp\left(\frac{9}{2}k^2 In^2\sigma\right) \quad (11)$$

If Eq. (11) is written for $k = 0$, 1, and 2, then v_g and σ can exactly be expressed in terms of the first three moments of the distribution according to the following relations:

$$In^2\sigma = \frac{1}{9}In\left(\frac{M_0 M_2}{M_1^2}\right) \quad \text{and} \quad v_g = \frac{M_1^2}{M_0^{3/2}M_2^{1/2}} \quad (12)$$

In this subsection, the ODEs describing the temporal evolution of the three leading moments of the size distribution for the free molecule size and continuum size regime are presented.

3.1.1. Free Molecule Size Regime

The ODE system that describes the spatio-temporal size distribution of the kth moment of the aerosol size distribution is computed by substituting Eq. (5) into Eq. (2), multiplying by v^k, and integrating over all particle sizes. That gives the temporal evolution of the zeroth moment which is affected by nucleation and coagulation:

$$\frac{dM_0}{dt} = -c_z\frac{dM_o}{dz} + I - B_2 b_0 \times (M_0 M_{1/6} + 2M_{1/3}M_{-1/6} + M_{2/3}M_{-1/2}) \quad (13)$$

where the coefficient b_0 is used for the relationship:

$$\left(\frac{1}{v}+\frac{1}{\tilde{v}}\right)^{1/2} = b_0\left(\frac{1}{v^{1/2}}+\frac{1}{\tilde{v}^{1/2}}\right) \quad (14)$$

and it was computed by the expression $b_0 = 0.633 + 0.092\sigma^2 - 0.022\sigma^3$ in publication of Pratisinis.[15] The evolution of M_1 (aerosol volume), which is affected by condensation is given by

$$\frac{dM_1}{dt} = -c_z\frac{(dM_1)}{dz} + Iv^* + B_1(S-1)M_{2/3} \quad (15)$$

And the second moment, M_2, depends on nucleation and coagulation according to the formula:

$$\frac{dM_2}{dt} = -c_z\frac{dM_2}{dz} + Iv^{*2} + 2B_1(S-1)M_{5/3} + 2b_2B_2(M_{7/6}M_1 + 2M_{4/3}M_{5/6} + M_{1/2}M_{5/3}) \quad (16)$$

where b_2 is used as b_0 but for coagulation kernel of the second moment b_2 is computed by the expression: $b_2 = 0.39 + 0.5\sigma - 0.214\sigma^2 + 0.029\sigma^3$ (Pratisinis[15]).

3.1.2. Continuum Size Regime

The spatio-temporal evolution of the kth moment of the aerosol size distribution in the continuum regime is computed by substituting Eq. (6) into Eq. (2), multiplying by v^k, and integrating over all particle sizes gives the temporal evolution of the zeroth moment M_0, M_1 and M_2

$$\frac{dM_0}{dt} = -c_z\frac{dM_0}{dz} + I - B_4\left[M_0^2 + M_{1/3}M_{-1/3} + B_5\lambda\left(\frac{4\pi}{3}\right)^{1/3} \times (M_0M_{-1/3} + M_{1/3}M_{-2/3})\right] \quad (17)$$

$$\frac{dM_1}{dt} = -c_z\frac{dM_1}{dz} + Iv^* + B_3(S-1)M_{1/3} \quad (18)$$

$$\frac{dM_2}{dt} = -c_z\frac{dM_2}{dz} + Iv^{*2} + 2B_3(S-1)M_{4/3} + 2B_4\left[M_1^2M_{4/3}M_{2/3} + B_5\lambda\left(\frac{4\pi}{3}\right)^{1/3} \times (M_1M_{2/3} + M_{1/3}M_{4/3})\right] \quad (19)$$

4. ANALYSIS OF RESULTS AND DISCUSSION

This section describes the application of moment model of the aerosol flow reactor for the purposes of nonlinear control of the reactor. Under the assumption of lognormal aerosol size distribution, the mathematical model that describes the evolution of the first three moments of distribution, together with the monomer and reactant concentration and temperature takes the following form.

$$\frac{dN}{d\theta} = -c_{zl}\frac{dN}{d\bar{z}} + I' - \xi N^2$$

$$\frac{dV}{d\theta} = -c_{zl}\frac{dV}{d\bar{z}} + I'k^* + \eta(S-1)N$$

$$\frac{dV_2}{d\theta} = -c_{zl}\frac{dV_2}{d\bar{z}} + I'k^{*2} + 2\varepsilon(S-1)V + 2\zeta V^2$$

$$\frac{dS}{d\theta} = -c_{zl}\frac{dS}{d\bar{z}} + C\bar{C}_1\bar{C}_2 - I'k^* - \eta(S-1)N$$

$$\frac{d\bar{C}_1}{d\theta} = -c_{zl}\frac{d\bar{C}_1}{d\theta} - A_1\bar{C}_1\bar{C}_2$$

$$\frac{d\bar{C}_2}{d\theta} = -c_{zl}\frac{d\bar{C}_2}{d\theta} - A_2\bar{C}_1\bar{C}_2$$

$$\frac{d\bar{T}}{d\theta} = -v_{zl}\frac{d\bar{T}}{d\bar{z}} + B\bar{C}_1\bar{C}_2\bar{T} + E\bar{T}(\bar{T}_w - \bar{T}) \quad (20)$$

$$\xi = \frac{\xi_{FM}\xi_C}{\xi_{FM}+\xi_C}$$

$$\xi_C = K\left[1 + \exp(In^2\sigma) + B_5(K_{n_1}/r_g') \times \exp\left(\frac{1}{2}In^2\sigma\right)(1+\exp(2In^2\sigma))\right]$$

$$\xi_{FM} = r_g'^{1/2}b_0\left[\exp\left(\frac{25}{8}In^2\sigma\right) + 2\exp\left(\frac{5}{8}In^2\sigma\right) + \exp\left(\frac{1}{8}In^2\sigma\right)\right] \quad (21)$$

$$\eta = \frac{\eta_{FM}\eta_C}{\eta_{FM}+\eta_C}, \quad \eta_{FM} = v_g'^{2/3}\exp(2In^2\sigma) \quad \text{and}$$

$$\eta_C = \frac{4K_{n_1}}{3}v_g'^{1/3}\exp\left(\frac{1}{2}In^2\sigma\right) \quad (22)$$

$$\varepsilon = \frac{\varepsilon_{FM}\varepsilon_C}{\varepsilon_{FM}+\varepsilon_C}, \quad \varepsilon_C = \frac{4K_{n_1}}{3}v_g'^{1/3}\exp\left(\frac{7}{2}In^2\sigma\right) \quad \text{and}$$

$$\varepsilon_{FM} = v_g'^{2/3}\exp(8In^2\sigma) \quad (23)$$

$$\zeta = \frac{\zeta_{FM}\zeta_C}{\zeta_{FM}+\zeta_C}$$

Table I. Dimensionless variables by Ashish and Panagioti.

$N = M_0/n_s$, $V = M_1/n_s v_1$	Aerosol concentration and volume
$V_2 = M_2/n_s v_1^2$	Second aerosol moment
$\tau = (2\pi m_1/k_B T)^{1/2} n_s s_1$	Characteristic time for particle growth
$K = (2k_B T/3\mu) n_s \tau$, $I' = I/(n_s/\tau)$	Coagulation coefficient and nucleation rate
$K_{n_1} = \lambda/r_1$	Knudsen number
$v_g' = v_g/v_1$, $r_g' = r_g/r_1$	Geometric volume and geometric radius
$\bar{z} = z/L$	Dimensionless distance
$c_{zl} = \tau c_z/L$, $\theta = t/\tau$	Dimensionless velocity and time

$$\zeta_{FM} = r_g'^{1/2} b_2 \exp\left(\frac{3}{2} In^2\sigma\right) \times \left[\exp\left(\frac{25}{8} In^2\sigma\right) + 2\exp\left(\frac{5}{8} In^2\sigma\right) + \exp\left(\frac{1}{8} In^2\sigma\right)\right]$$

$$\zeta_C = K\left[1 + \exp(In^2\sigma) + B_5(K_{n_1}/r_g') \times \exp\left(-\frac{1}{2} In^2\sigma\right)(1 + \exp(-2In^2\sigma))\right] \quad (24)$$

where $\bar{C}_1$ and $\bar{C}_2$are the dimensionless concentrations of the reactants, $\bar{T}_w$, $\bar{T}$ are the dimensionless reactor and wall temperature, respectively, A_1, A_2, B, C, E are the dimensionless quantities. See Table I for dimensionless variables. Table II gives the process parameters used in the simulation.

Dimensionless quantities for the model of Eq. (20), according to Ashish and Panagiotis[14]

$$A_1 = \tau k P_0 y_{20}/RT_0, \quad A_2 = \tau k P_0 y_{10}/RT_0$$

$$B = P_0 k\tau \Delta H_R y_{10} y_{20}/RT_0^2 C_P, \quad \bar{C}_i = y_i/y_{10}\bar{T}$$

$$C = N_{av} k\tau y_{10} y_{20} (P_0/RT_0)^2/n_{s0}, \quad E = 4URT_0\tau/DC_p P_0$$

$$\bar{T} = T/T_0 \quad \text{and} \quad \bar{T}_w = T_w/T_0$$

Table II. Process model parameters for the simulation study.

$L = 20$ m, $D = 0.05$ m	Reactor length and diameter
$P_0 = 1$ atm	Process pressure
$T_0 = 350$ K	Inlet temperature
$T_w = 250$ K–600 K	Wall temperatures
$y_{10} = y_{20} = 40$ ppm	Inlet mole fractions of reactants
$U = 10.4$ Jm^{-2}s^{-1} K^{-1}	Overall coefficient of heat transfer
$\Delta H_R = 175.7$ KJ mol^{-1}	Heat of reaction
$C_P = 29.1$ J mol^{-1} K^{-1}	Heat capacity of process fluid
$MW_g = 14.0 \times 10^{-3}$ kg mol^{-1}	Mol wt. of process fluid
$K = 11.4$ m^3 mol^{-1}s^{-1}	Reaction rate constant
$\mu = 3.5 \times 10^{-6}$ kg m^{-1}s^{-1}	Viscosity of process fluid
$\log P_s(mmHg) = -4{,}644/T$	PVT relation
$+0.906 \log T - 0.00162T + 9.004$	PVT relation
$\gamma = 0.08$ Nm^{-1}	Surface tension
$v_1 = 5.33 \times 10^{-29}$ m^3	Monomer volume
$N_{av} = 6.023 \times 10^{23}$# mol^{-1}	Avogrado's constant
$R = 8.314$ J mol^{-1}K^{-1}	Universal gas constant
$k_B = 1.38 \times 10^{-23} J$ K^{-1}	Boltzmann's constant

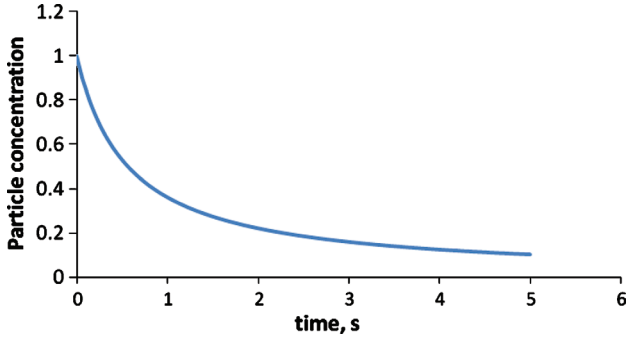

Fig. 1. Steady state profile of dimensionless particle number concentration.

Figures 1 and 2 shows the steady state profile of dimensionless particle number concentration, N and volume v as a function of time. As particles collide and coagulate, their number concentration decreases. This is revealed in the zeroth moment M_0. As the flow evolves, M_0 decreases while the particle volume is increasing. Since the control objective is to control nanoparticle growth with desired particle distribution in high temperature reactor, we also study the effect of wall temperature on average particle diameter. It is a variable that could be used in industry to control the aerosol size distribution.

Figures 3 and 4 shows the distribution of Average particle diameter and surface area with process time. Particle

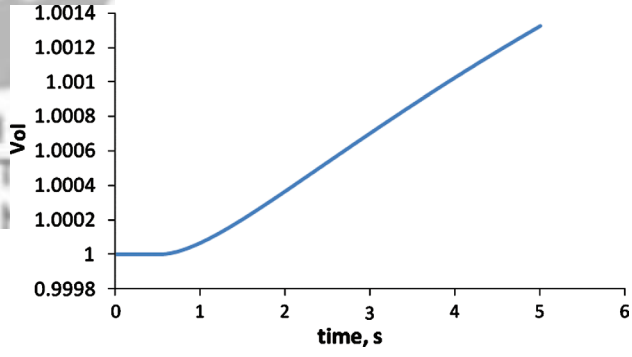

Fig. 2. Steady state profile of dimensionless volume.

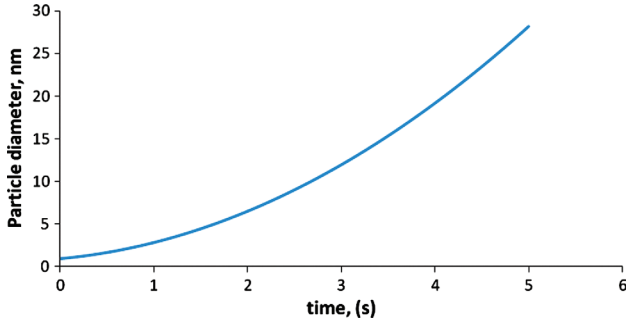

Fig. 3. Average particle diameter against time.

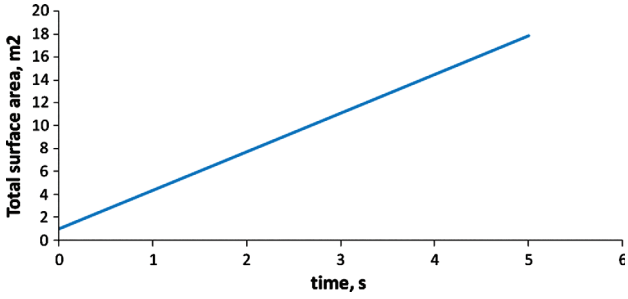

Fig. 4. The total surface area against time.

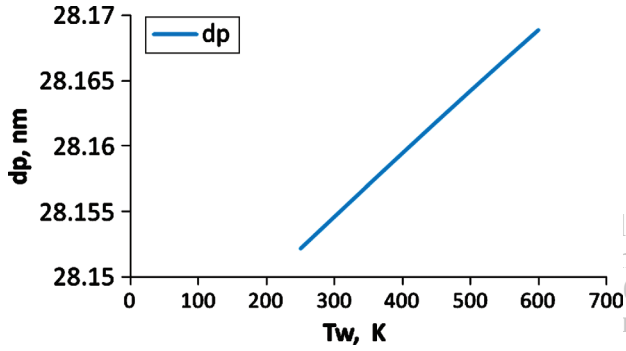

Fig. 5. Average particle diameter as function of the wall temperature.

diameter in the reactor increases with increase of the process time and the total surface area increases due to coagulation. One can see from the graphs that when particles are nucleated, a primary particle with diameter less than 2nm is produced. After a certain number of particles have been produced, the frequency of bi-particle collision increases, resulting in a sharp increase in particle diameter.

Figure 5 gives the plot of the average particle diameter, d_p versus the wall temperature. From the Figure 5, it is clear that the wall temperature is a variable that has significant effect on the average particle diameter.

In the numerical investigation of the reactor wall temperature on particle growth was found that the particle size increases with increasing wall temperature.

5. CONCLUSIONS

Under the assumption of lognormal size distribution, the method of moment was employed to reduce the population balance model into the simpler model, describing the evolution of the first three leading moment. This simplified model is a set of ODEs. The average particle diameter can be increased by increasing the reactor wall temperature. Based on the sensitivity of wall temperature upon the particle diameter d_p, the model can be used as a basis to synthesize a feedback controller which manipulates the wall temperature of the reactor to control the aerosol size distribution at the outlet of the reactor.

References

1. D. C. Panagiotis, Model–Based Control of Particulate Process, Springer, New York **(2002)**.
2. D. Ramkrishna and A. W. Mahoney, *Chem. Eng. Sci.* 57, 595 **(2002)**.
3. K. F. Sheldon, Smoke, Dust, and Haze: Fundamentals of Aerosol Dynamics, 2nd edn., Oxford University Press, New York **(2000)**
4. D. C. Panagiotis, E. F. Nael, L. Mingheng, and M. Prashant, *Chem. Engng. Sci.* 63, 1156 **(2008)**
5. Y. H. Debra and M. K. Sonia, *J. Atm. Env.* 32, 1701 **(1998)**.
6. K. Ashish and D. C. Panagiotis, *Com. Chem. Engng.* 26, 1153 **(2002)**.
7. A. T. Suddha and T. M. Mark, *Aerosol Sci.* 35, 889 **(2004)**.
8. B. James and D. C. Panagiotis, *Int. J. Cont.* 73, 439 **(2000)**.
9. A. H. Aleck and A. K. Costas, *J. Chem. Engng. Sci.* 60, 4157 **(2005)**.
10. M. K. Akhtar, G. Lipscomb, and S. E. Prantsinis, *Aerosol. Sci. Tech.* 21, 83 **(1994)**.
11. C. A. Dorao and H. A. Jakobsen, *Com. Chem. Engng.* 30, 535 **(2006)**.
12. J. A. Schwarz, C. I. Contescu, and K. Putyera, Dekker Encyclopedia of Nanoscience and Technology, 1st edn., Mercel Dekker, New York **(2004)**.
13. S. Dan, H. E. F. Nael, L. Mingheng, M. Prashant, and D. C. Panagiotis, *Chem. Engng. J.* 6, 268 **(2006)**.
14. K. Ashish and D. C. Panagiotis, *Chem. Engng. Sci.* 54, 2669 **(1999)**.
15. S. E. Pratsinis, J. Collide. *Interface Sci.* 124, 416 **(1988)**.
16. K. Ashish and D. C. Panagiotis, *Aerosol Sci. Tech.* 32, 369 **(2000)**.

Received: 6 April 2009. Accepted: 24 April 2009.